

Ultra-High Temperature Ceramics for Hypersonic Vehicles - Testing and Characterization

Mr.G.Dhanajayan

Assistant Professor,

Dept. of Aeronautical Engineering
MLRIT, Hyderabad.

L.Swathi

M.Tech Student,

Dept. of Aeronautical Engineering
MLRIT, Hyderabad.

Dr. M Satyanarayana Gupta

Professor & HoD,

Dept. of Aeronautical Engineering
MLRIT, Hyderabad.

ABSTRACT

Ultra High Temperature Ceramics (UHTCs) are good choices for several extreme applications: thermal protection materials on hypersonic aerospace vehicles or re-usable atmospheric re-entry vehicles, specific components for propulsion, furnace elements, refractory crucibles, etc. Hypersonic flights, re-entry vehicles, and propulsion applications all require new materials that can perform in oxidizing or corrosive atmospheres at temperatures in excess of 2000°C and sometimes over the course of a long working life. Ultra High Temperature Ceramics (UHTCs) are good candidates to fulfil these requirements. This family of ceramic compounds is made of borides, carbides and nitrides such as ZrB₂, HfB₂, which are characterized by high melting points, high hardness, chemical inertness and relatively good resistance to oxidation in severe environments. For hypersonic vehicles with sharp aero surfaces (engine cowl inlets, wing leading edges and nose caps), there are foreseeable needs for materials that can withstand temperatures of 2000 to 2400°C, operate in air and be re-usable. At present, the structural materials for use in high temperature oxidizing environments are limited to SiC and Si₃N₄ based materials, oxide ceramics and C/C composites with thermal protection. Silicon-based ceramics and protected C/C composites exhibit good oxidation resistance, but only up to ~1600°C, and their thermal cycling lifetimes are modest. The development of structural materials for use in oxidizing and rapid heating environments at temperatures above 1600°C is therefore of great importance for engineering.

INTRODUCTION

The development of ultra-high temperature ceramics for aerospace applications continues around the globe. While significant progress has been made in recent years in understanding fundamental microstructure-processing-property relationships in these materials, further work is needed to develop UHTCs for

applications such as sharp leading edges for hypersonic aerospace vehicles Ultra-High Temperature Ceramics - An Introduction to Ultra-High Temperature Ceramics and propulsion components for rocket motors. Development is likely to be driven by "market pull" based on applications where performance requirements necessitate the use of ceramics due to some combination of temperature requirements, weight savings compared to heavier refractory metals, or use of simpler passive designs as opposed to more complex actively cooled components.

LITERATURE SURVEY

Introduction to ultra-high temperature ceramic compounds (UHTCC)

There exists great interest in the development of materials that tolerate very high temperatures (>1600 °C), high pressures (> 50 KPa), strong localized stresses (mechanical contact and wear), and chemically aggressive environments (corrosive gases). Among the industries interested in these materials are the aeronautics and space sectors. Indeed, it is expected that the XXI century will see a revolution in supersonic and space flight, and in general the development of propulsion craft. Without a doubt, all these advances, as has been the case up to now, will be intimately related with the development of new materials.

With respect to supersonic flights, it is sufficient to consider that as the speed of the craft increases, the temperature of its surface grows exponentially due to the high friction. The speed forecasts are already for Mach 6, for which reason the estimated temperatures are greater than 1500 °C, as well as very severe wear of the surfaces. Therefore, one of the present challenges in supersonic technology is the manufacture of light materials that are resistant to oxidation, wear, thermal shock, and creep in conditions of cyclic and prolonged use at high temperatures.

Space shuttles are re-usable vehicles for exit and entry into the atmosphere. When returning to Earth, the nose and wing tips reach temperatures greater than 1700 °C. In order to reduce those high temperatures designs with blunt shapes are used, so that the shock wave induced during re-entry turns aside part of the generated heat 2.1&2.2. Hence, the technical challenges are nowadays centered on the development of high temperature materials that allow the manufacture of light components that are more resistant to oxidation, damage by contact, wear, thermal shock, and creep.

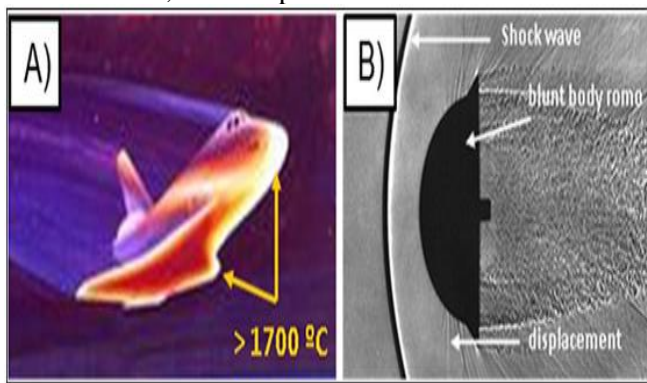


Fig 2.1 Image of a space shuttle returning to Earth & 2(b) shock wave generated during the re-entry to the atmosphere.

Ultra-high-temperature ceramics' (UHTCs) are a class of refractory ceramics that offer excellent stability at temperatures exceeding 2000 °C being investigated as possible thermal protection system (TPS) materials, coatings for materials subjected to high temperatures, and bulk materials for heating elements. Broadly speaking, UHTCs are borides, carbides, nitrides, and oxides of early transition metals. Current efforts have focused on heavy, early transition metal borides such as hafnium diboride (HfB₂) and zirconium diboride (ZrB₂), additional UHTCs under investigation for TPS applications include hafnium nitride (HfN), zirconium nitride (ZrN), titanium carbide (TiC), titanium nitride (TiN), thorium dioxide (ThO₂), tantalum carbide (TaC) and their associated composites.

Thermodynamic properties

In comparison with carbide and nitride-based ceramics, diboride-based UHTCs exhibit higher thermal conductivity (refer to Table 2.2), where we can see that hafnium diboride has thermal conductivity of 105, 75, 70 W/m²K at different temperature while hafnium carbide and nitride have values only around

20 W/m²K. Thermal shock resistance of HfB₂ and ZrB₂ was investigated by Man Labs and it was found that these materials did not fail at thermal gradients sufficient for the failure of SiC; indeed, it was found that hollow cylinders could not be cracked by an applied radial thermal gradient without first being notched on the inner surface. UHTCs generally exhibit thermal expansion coefficients in the range of 5.9–8.3×10⁻⁶K⁻¹. The structural and thermal stability of ZrB₂ and HfB₂ UHTCs results from the occupancy of bonding and anti-bonding levels in hexagonal MB₂ structures with alternating hexagonal sheets of metal and boride atoms.

In such structures, the principal frontier electronic states are bonding and anti-bonding orbitals resulting from bonding between boron 2p orbitals and metal d orbitals; before group (IV), the number of available electrons in a unit cell is insufficient to fill all bonding orbitals, and beyond it they begin to fill the anti-bonding orbitals. Both effects reduce the overall bonding strength in the unit cell and therefore the enthalpy of formation and melting point. Experimental evidence shows that as one moves across the transition metal series in a given period, the enthalpy of formation of MB₂ ceramics increases and peaks at Ti, Zr, and Hf before decaying as the metal gets heavier. As a result, the enthalpies of formation of several important UHTCs are as follows: HfB₂> TiB₂> ZrB₂> TaB₂> NbB₂> VB₂.

Mechanical properties

Table 2.3 lists UHTC carbides and borides mechanical properties. It is extremely important that UHTCs are able to retain high bending strength and hardness at high temperatures (above 2000 °C). UHTCs generally exhibit hardness above 20 GPa due to the strong covalent bonds present in these materials. However, the different methods of processing UHTCs can lead to great variation in hardness values.

UHTCs exhibit high flexural strengths of > 200 MPa at 1800 °C, and UHTCs with fine-grained particles exhibit higher flexural strengths than UHTCs with coarse grains. It has been shown that diboride ceramics synthesized as a composite with silicon carbide (SiC) exhibit increased fracture toughness (increase of 20% to 4.33 MPam^{1/2}) relative to the pure diborides. This is due to material densification and a reduction in grain size upon processing.

Table 2.3 Flexural strength, hardness, and Young's Modulus at given temperatures for selected UHTCs

Material	Temperature (°C)	Young's Modulus (GPa)	Flexural Strength (MPa)	Hardness (GPa)
HfB ₂	23	530	480	21.2–28.4
–	800	485	570	–
–	1400	300	170	–
–	1800	–	280	–
HfB ₂ -20%SiC	23	540	420	–
–	800	530	380	–
–	1400	410	180	–
–	1800	–	280	–
ZrB ₂	23	500	380	28.0
–	800	480	430	–
–	1400	360	150	–
–	1800	–	200	–
ZrB ₂ -20%SiC	23	540	400	–
–	800	500	450	–
–	1400	430	340	–
–	1800	–	270	–
TaB ₂	23	257	–	25.0
TiB ₂	23	551	370	33.0
HfC	23	352	–	26.0
ZrC	23	348	–	27.0
TiC	23	451	–	30.0
TaC	23	285	–	18.2
SiC	23	415	359	32
–	1000	392	397	8.9

Synthesis of diboride (Zr, Hf, and Ti) UHTCs

UHTCs possess simple empirical formulas and thus can be prepared by a wide variety of synthetic methods. UHTCs such as ZrB₂ can be synthesized by stoichiometric reaction between constituent elements,

in this case Zr and B. This reaction provides for precise stoichiometric control of the materials.

At 2000 K, the formation of ZrB₂ via stoichiometric reaction is thermodynamically favorable ($\Delta G = -279.6$ kJ mol⁻¹) and therefore, this route can be used to produce ZrB₂ by self-propagating high-temperature synthesis (SHS). This technique takes advantage of the high exothermic energy of the reaction to cause high temperature, fast combustion reactions. Advantages of SHS include higher purity of ceramic products, increased sinter ability, and shorter processing times. However, the extremely rapid heating rates can result in incomplete reactions between Zr and B, the formation of stable oxides of Zr, and the retention of porosity. Stoichiometric reactions have also been carried out by reaction of attrition milled (wearing materials by grinding) Zr and B powder (and then hot pressing at 600 °C for 6 h), and Nano scale particles have been obtained by reacting attrition milled Zr and B precursor crystallites (10 nm in size).

Unfortunately, all of the stoichiometric reaction methods for synthesizing UHTCs employ expensive charge materials, and therefore these methods are not useful for large-scale or industrial applications.

Applications

UHTCs, specifically Hf and Zr based diboride, are being developed to handle the forces and temperatures experienced by leading vehicle edges in atmospheric reentry and sustained hypersonic flight. The surfaces of hypersonic vehicles experience extreme temperatures in excess of 2500 °C while also being exposed to high-temperature, high-flow-rate oxidizing plasma. The material design challenges associated with developing such surfaces have so far limited the design of orbital re-entry bodies and hypersonic air-breathing vehicles such as scramjets and DARPA's HTV (Hypersonic Technology Vehicle) because the bow shock in front of a blunt body protects the underlying surface from the full thermal force of the onrushing plasma with a thick layer of relatively dense and cool plasma. Sharp edges dramatically reduce drag, but the current generations of thermal protection system materials are unable to withstand the considerably higher forces and temperatures experienced by sharp leading edges in reentry conditions. The relation between radius of curvature and temperature in a leading edge is inversely

proportional, e.g. as radius decreases temperature increases during hypersonic flight. Vehicles with "sharp" leading edges have significantly higher lift to drag ratios, enhancing the fuel efficiency of sustained flight vehicles such as DARPA's HTV-3 and the landing cross-range and operational flexibility of reusable orbital space plane concepts being developed such as the Reaction Engines Sky Lon and Boeing X-33.

Zirconium diboride is used in many boiling water reactor fuel assemblies due to its refractory nature, corrosion resistance, high-neutron-absorption cross-section of 759 barns, and stoichiometric boron content. Boron acts as a "burnable" neutron absorber because its two isotopes, 10B and 11B, both transmute into stable nuclear reaction products upon neutron absorption (4He + 7Li and 12C, respectively) and therefore act as sacrificial materials which protect other components which become more radioactive with exposure to thermal neutrons. However, the boron in ZrB₂/ZrB₂ must be enriched in 11B because the gaseous helium evolved by 10B strains the fuel pellet of UO₂ creates a gap between coating and fuel, and increases the fuel's centerline temperature; such cladding materials have been used on the uranium oxide fuel pellets in Westinghouse AP-1000 nuclear reactors.

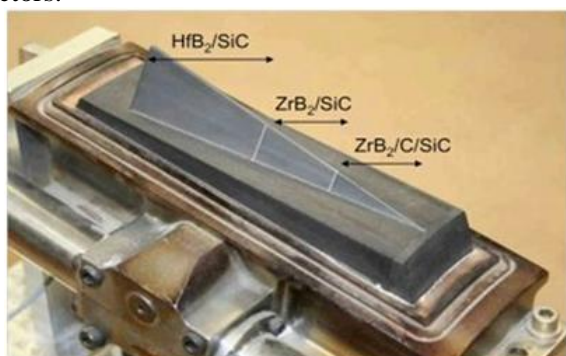


Fig. 2.2 Image of shock wave generated during the re-entry to the atmosphere.

INTRODUCTION TO ZIRCONIUM DIBORIDE

Ultra-high temperature ceramics (UHTCs) are a class of materials that can be used in environments that exhibit extremes in temperature, chemical reactivity, erosive attack, etc. Extreme environments could be considered as being encountered in applications including handling of molten metals and electrodes for electric arc furnaces, but this article will focus on materials being examined for aerospace applications

such as hypersonic flight, scramjet propulsion, rocket propulsion, and atmospheric re-entry.



Fig. 3.1 Conceptual design for the X43-A, a reusable hypersonic aerospace vehicle that would utilize UHTC leading edges and control surfaces

A variety of criteria can be used to define UHTCs including ultimate use temperature, environmental resistance, and strength at elevated temperature. For this article, UHTCs are defined as compounds with melting temperatures in excess of 3000°C. Using the melting temperature criterion, only a few materials can be classified as UHTCs, most of which are borides, carbides, or nitrides of early transition metals. Table 3.1 lists some compounds that meet the melting temperature criterion.

From the 1950s through about 1970, many of these compounds were studied extensively in the U.S. and U.S.S.R. for potential aerospace applications. After a period of relative inactivity, research on UHTCs has experienced resurgence in recent years with significant efforts in countries including China, Japan, Italy, Ukraine, and the United States, among others.

Table 3.1 UHTC compound materials

Compound	Melting Temperature(°C)
TiB ₂	3225
ZrB ₂	3247
NbB ₂	3036
HfB ₂	3380
TaB ₂	3037
TiC	3067
ZrC	3445
NbC	3610
HfC	3928

Zirconium

Zirconium is a lustrous, greyish-white, soft, ductile and malleable metal which is solid at room temperature, though it becomes hard and brittle at lower purities. In powder form, zirconium is highly flammable, but the solid form is far less prone to ignition. Zirconium is highly resistant to corrosion by alkalis, acids, salt water and other agents. However, it will dissolve in hydrochloric and sulfuric acid, especially when fluorine is present.

Alloys with zinc become magnetic below 35 K. Zirconium's melting point is 1855 °C (3371 °F), and its boiling point is 4371 °C (7900 °F). Zirconium has an electronegativity of 1.33 on the Pauling scale. Of the elements within d-block, zirconium has the fourth lowest electronegativity after yttrium, lutetium and hafnium. At room temperature zirconium exhibits a hexagonally close packed crystal structure, α-Zr, which changes to β-Zr a body-centered cubic crystal structure at 863 °C. Zirconium exists in the β-phase until the melting point.

Processing

Two grades of commercially available ZrB₂ were used in this study. The smaller particle size ZrB₂ powder had a purity of >99% (metals basis) and a reported starting particle size of 2 μm. The larger particle size powder had a purity of >99% and a reported starting particle size of 6 μm. The SiC powder was predominantly α-SiC, and it had a reported purity of 98.5% and a particle size of 0.7 μm. Batches containing 70 vol% ZrB₂ and 30 vol% SiC were prepared. To reduce particle size and promote intimate mixing, the batches were attrition milled. For milling, a 750 ml fluoro polymer-coated bucket was charged with ~250 ml hexane, ~150 g of powder, and ~3000 g of Co-bonded WC milling media (~3.5 mm diameter). Powders were milled at 600 rpm for 2 h. To minimize segregation by sedimentation during drying, solvent removal was performed using rotary evaporation at a temperature of 70°C, a vacuum of 200 mmHg (~27 kPa), and a rotation speed of 150 rpm.

Milled powders were hot-pressed in graphite dies lined with graphite foil and coated with BN. Each of the different powder mixtures was hot-pressed at 1850, 1950 or 2050°C for 45 min at a pressure of 32 MPa. In addition, the mixture prepared from ZrB₂ with an initial particle size of 2 μm was hot pressed at 2050°C

for 90 and 180 min at 32 MPa. After loading the powder into the dies, the furnace was heated at an average rate of ~10°C/min to the hot pressing temperature. The powders were heated in vacuum (~150 mTorr) up to 1650°C at which time the atmosphere was switched to flowing argon. A detailed description of the temperature ramp used to prepare the specimens has been reported previously. Above ~800°C, the temperature of graphite die was monitored using an infrared thermometer. When the die temperature reached the hold temperature, a uniaxial load of 32 MPa was applied.

The furnace was cooled at ~20°C/min to room temperature when the hot pressing time (45, 90, or 180 min) had elapsed. The load was removed when the die temperature dropped below 1750°C. Each billet was assigned a code to designate the grade of ZrB₂ (A or B), the hot-pressing temperature (1850, 1950, or 2050°C), and the hot pressing time (45, 90, or 180 min) as summarized in Table 4.1. Two billets were prepared for each combination of ZrB₂ grade, hot pressing temperature, and hot pressing time. Each billet had a diameter of ~40 mm and thickness of ~5 mm.

Table 4.1 Results of hot processing process

Material	ZrB ₂ grade	Temperature (°C)	Time (min)	Abbreviation
ZrB ₂ -SiC	A	1850	45	A-1850-45
ZrB ₂ -SiC	A	1950	45	A-1950-45
ZrB ₂ -SiC	A	2050	45	A-2050-45
ZrB ₂ -SiC	B	1850	45	B-1850-45
ZrB ₂ -SiC	B	1950	45	B-1950-45
ZrB ₂ -SiC	B	2050	45	B-2050-45
ZrB ₂ -SiC	B	2050	90	B-2050-90
ZrB ₂ -SiC	B	2050	180	B-2050-180

Table 5.1 Results of young's modulus

Material	E (GPa)	Number of strength bars
A-1850-45	503 ± 6	9
A-1950-45	501 ± 1	11
A-2050-45	503 ± 1	9
B-1850-45	516 ± 3	10
B-1950-45	507 ± 3	11
B-2050-45	505 ± 2	11
B-2050-90	508 ± 4	11
B-2050-180	505 ± 1	12

Table 6.1 Results for hardness

Material	H (GPa)	Number of strength bars
A-1850-45	22 ± 2	9
A-1950-45	22 ± 2	11
A-2050-45	23 ± 2	9
B-1850-45	20 ± 2	10
B-1950-45	22 ± 2	11
B-2050-45	23 ± 1	11
B-2050-90	22 ± 1	11
B-2050-180	22 ± 1	12

Table 7.1 Results for fracture toughness

Material	K _{IC} (MPa m ^{1/2})	Number of strength bars
A-1850-45	3.9 ± 0.1	9
A-1950-45	4.0 ± 0.2	11
A-2050-45	4.3 ± 0.2	9
B-1850-45	5.5 ± 0.3	10
B-1950-45	5.2 ± 0.4	11
B-2050-45	4.3 ± 0.2	11
B-2050-90	4.2 ± 0.1	11
B-2050-180	4.5 ± 0.2	12

RESULTS

Table 9.1 Measured modulus of elasticity, hardness, fracture toughness, and four points bend strength for ZrB₂-30% SiC

CONCLUSION AND FUTURE SCOPE

Billets of ZrB₂ containing 30 volume percent SiC particulate additions were produced by hot pressing two different grades of commercial ZrB₂ powders. Analysis by SEM revealed a uniform dispersion of SiC particulates in the ZrB₂ matrix of all of the materials. Hardness and elastic modulus were not affected by different processing conditions and showed an average value of ~22 and 505 GPa, respectively. In contrast, fracture toughness and strength were found to depend on hot pressing temperature as well as the initial particle size of the ZrB₂ precursor. Fracture toughness values were analyzed using a model that suggested that the size and distribution of SiC could potentially affect toughness by altering the amount of crack deflection. Specifically, analysis suggested that the largest SiC grains in the microstructure acted as the critical flaw causing the failure of the specimen. Hence, smaller SiC grain sizes would result in even higher strengths for ZrB₂-SiC.

Further tests for re-entry conditions (more cycles, oxidizing atmosphere). Sensitivity to thermal shock

resistance (internal mechanical stresses) for ceramic materials.

REFERENCES

- [1]. Monteverde F, Bellosi A (2004) *AdvEng Mater* 6:331
- [2]. Kolodziej P. Aerothermal performance constraints for hypervelocity small radius un swept leading edges and nosetips. NASA Technical Memorandum 1122204
- [3]. Walker SP, Sullivan BJ (2003) Paper AIAA-2003-6915. Published in the proceedings of the 12th AIAA international space planes and hypersonic systems and technologies conference, American Institute of Aeronautics and Astronautics, Norfolk, VA, December 15–19
- [4]. Levine SR, Opila EJ, Halbig MC, Kiser JD, Singh M, Salem JA (2002) *J Eur Ceram Soc* 22:2757
- [5]. Chamberlain AL, Fahrenholtz WG, Hilmas GE, Ellerby DT (2004) *J Am Ceram Soc* 87:1170
- [6]. Chamberlain AL, Fahrenholtz WG, Hilmas GE, Ellerby DT (2004) *Key Eng Mater* 493:264–268
- [7]. Van Wie DM, Drewry DG Jr, King DE, Hudson CM (2004) *J Mater Sci* 39:5915
- [8]. Monteverde F, Bellosi A (2003) *J Electrochem Soc* 150:B552
- [9]. Monteverde F, Bellosi A, Guicciardi S (2002) *J Eur Ceram Soc* 22:279
- [10]. Rieck U, Bolz J, Muller-Wiesner D (1995) *Int J Mater Prod Tec* 10:303
- [11]. Kochendorfer R. International symposium for light weight structures proceedings, ESTEC, Noordwijk, The Netherland, 25–27 March, 1992 (ESA SP-336, October 1992), p 7
- [12]. Fahrenholtz WG, Hilmas GE, Chamberlain AL, Zimmermann JW (2004) *J Mater Sci* 39:5951
- [13]. Kuwabara K, Sakamoto S, Kida O, Ishino T, Kodama T, Nakajima H, Ito T, Hirakawa Y (2005) Proceedings of international conference on refractories, UNITECR'03 Osaka, Japan, p 302
- [14]. Kinoshita S, Yoshimasa Y, Ono Y (2003) Proceedings of international conference on refractories, UNITECR'03, Osaka, Japan, p 205
- [15]. Prietzel S, Hunold K, Potscke J, Kross U (2001) Proceedings of international conference on refractories, UNITECR'01, Cancun, Mexico, p 983
- [16]. Kaji N, Shikano H, Tanaka I (1992) *Taikabutsu Overseas* 14:39
- [17]. Norasethekul S, Eubank PT, Bradley WL, Bozkurt B, Stucker B (1999) *J Mater Sci* 34:1261
- [18]. Upadhya K, Yang J-M, Hoffman WP (1997) *Am Ceram Soc Bull* 58:51
- [19]. Mroz C (1994) *Am Ceram Soc Bull* 73:141
- [20]. Zhang G-J, Deng Z-Y, Kondo N, Yang J-F, Ohji T (2000) *J Am Ceram Soc* 83:2330
- [21]. Goldstein A, Gefen Y, Goldenberg A (2001) *J Am Ceram Soc* 84:642
- [22]. Zhang GJ, Ando M, Yang JF, Ohji T, Kanzaki S (2004) *J Eur Ceram Soc* 24:171
- [23]. Nishida A, Shimamura T, Kohtoku Y (1990) *J Ceram Soc Jpn* 98:412
- [24]. O YT, Koo JB, Hong KJ, Park JS, Shin DC (2004) *Mater Sci Eng A* 374:191
- [25]. Koyama T, Nishiyama A, Niihara K (1994) *J Mater Sci* 29:3949
- [26]. Mishra SK, Das SK, Ray AK, Ramachandrarao P (2002) *J Am Ceram Soc* 85:2846
- [27]. ASTM C 1259-01 (2005) ASTM book of standards. ASTM International, West Conshohocken, PA
- [28]. ASTM C 1161-02c (2005) ASTM book of standards. ASTM International, West Conshohocken, PA

[29]. Chantikul P, Anstis GR, Lawn BR, Marshall DB (1981) J Am Ceram Soc 64:539

[30]. Wachtman JB (1996) Mechanical properties of ceramics. John Wiley & Sons Inc., New York

[31]. Chamberlain AL, Fahrenholtz WG, Hilmas GE (2006) J Am Ceram Soc 89:450

[32]. Cutler RA (1991) In: Schneider SJ Jr (ed) Ceramics and glasses, engineered materials handbook, vol 4. ASM International, Materials Park, OH, p 787

[33]. Shaffer PTB (1991) In: Schneider SJ Jr (ed) Ceramics and glasses, engineered materials handbook, vol 4. ASM International, Materials Park, OH, p 804

[34]. Ohji T, Jeong Y-K, Chao Y-H, Niihara K (1998) J Am Ceram Soc 81:1453

[35]. Wiederhorn SM (1984) Annu Rev Mater Sci 14:374

[36]. Ruhle M, Dalgleish BG, Evans AG (1987) ScrMetall Mater 21:681

[37]. Rice RW (1981) Ceram EngSciProc 2:661

[38]. Rice RW (1985) Ceram EngSciProc 6:589